Toughness Improvement of an Epoxy/Anhydride Matrix. Influence on Processing and Fatigue Properties of Unidirectional Glass–Fiber Composites

E. URBACZEWSKI-ESPUCHE,* J. F. GERARD, J. P. PASCAULT, G. REFFO, and H. SAUTEREAU

Laboratoire des Matériaux Macromoléculaires, URA CNRS n° 507, Institut National des Sciences Appliquées de Lyon, 20, Avenue A. Einstein, 69621 Villeurbanne Cedex, France

SYNOPSIS

Wet filament winding processing for unidirectional composites uses specific reactive systems with low viscosity and long-pot life. This work describes improvement of toughness of an epoxy/anhydride matrix using, first, the increasing of the average molecular weight of the diepoxy prepolymer and, second, the introduction of a functionalized elastomer. Thermomechanical behaviors (glass transition temperature, elasticity, plastic, and fracture properties) are discussed in terms of (1) the increase of the average molecular weight between crosslinks in the first case and (2) the amount of elastomer dissolved in the matrix in the second case. Dynamic mechanical spectroscopy confirms that phase separation occurred, during curing, between the epoxy system and the elastomer. A good correlation is obtained between matrix toughness and fatigue behavior of unidirectional composites.

INTRODUCTION

Epoxy networks are the most significant matrices used for filament winding. Detailed characterization of epoxy systems is important mostly for two reasons. The first one is obtaining systems having specific properties in relation with the processing mode and with the use of the composite structure. The second one is the understanding of the role of the matrix in fiber-based composites.

Wet filament winding processing requires reactive systems with low initial viscosity for fiber impregnation and long pot life for handling ease. An additional constraint lies within the industrial using conditions of the composites. In our case, the composites must have a good thermal resistance up to 100°C in addition to a good fatigue behavior. To achieve this objective, a wide range of epoxide systems have been formulated. The system described here contains two monomers: diglycidyl ether of bisphenol A (DGEBA) and methyl tetrahydrophthalic acid anhydride (MTHPA) with an imidazole as initiator. Compared to the epoxy–diamine systems formulated, the anhydride-based system has a longer pot life at low temperature associated to a higher activation energy ($\approx$ 80 kJ $\cdot$ mol^{-1}) and a higher reactivity at high temperature (Fig. 1).

In opposition to the commonly used diamine-based systems, an anhydride-based system does not require the use of an epoxy reactive diluent[1-3] or solvent because this comonomer has a low viscosity and its amount in the reactive system is high (more than 90% by weight of the epoxy prepolymer). Thus the initial viscosity level of the liquid reactive system is low, nevertheless too low to obtain an optimum fiber content by the wet filament winding process.

Thus the aim of this work is to optimize the anhydride-based system for filament winding by increasing the initial viscosity of the liquid reactive system and by improving the mechanical properties of the networks. Two ways are investigated in this paper.

— The use of DGEBA prepolymers with higher number average molecular weight. Their high

* To whom correspondence should be addressed at Laboratoire d'Etudes des Matériaux Plastiques et des Biomatériaux, URA CNRS n° 507, Université Claude Bernard Lyon I, 43, Boulevard du 11 Novembre 1918, 69622 Villeurbanne Cedex, France.

Journal of Applied Polymer Science, Vol. 47, 991–1002 (1993)
 CCC 0021-8995/93/060991-12

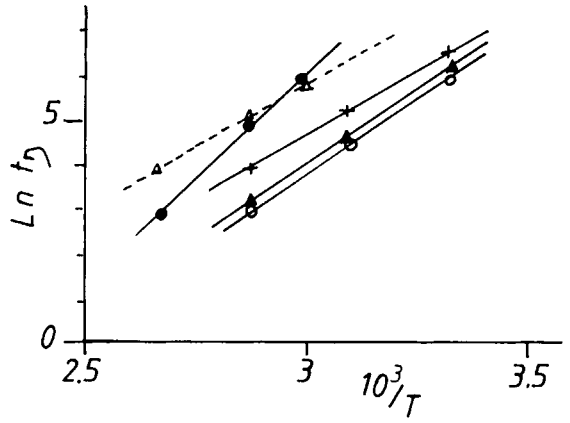

Figure 1 Arrhenius plot for the time t_η (time to reach 5000 Pa s) for the following systems: (●) DGEBA $\bar{n}$ = 0.03/MTHPA r = 0.85 + 1% MIA (MTHPA = methyl tetrahydrophthalic acid anhydride); (△) DGEBA $\bar{n}$ = 0.03/MDA r = 1 (MDA = methylene dianiline); (○) DGEBA $\bar{n}$ = 0.03/DCH r = 1 (DCH:1,2 diaminocyclohexane); (▲) DGEBA $\bar{n}$ = 0.03/IPD r = 1 (IPD = isophorone diamine) (×) DGEBA $\bar{n}$ = 0.03/3DCM r = 1 (3DCM = 3,3'-dimethyl 4,4'-diamine dicyclohexylmethane). For epoxy/amine systems r is the function ratio amine/epoxy.

viscosity will have a noticeable influence on the viscosity level of the liquid reactive system, and they could lead to an increase of the fracture energy.

The introduction of an initially miscible carboxy or epoxy-terminated butadiene-acrylonitrile rubber. Generally the viscosity of this type of rubbers is higher than 60 Pa · s at 25°C, and they are known to lead to an improvement of the impact resistance of the networks by a phase separation phenomenon during curing.[4]

In this study, we investigated the effects of these two kinds of modifications on the properties of the matrices but also on the fatigue behavior of the unidirectional glass fiber composites.

EXPERIMENTAL

Materials

Figure 2 and Table I display the structural formulæ and the characteristics of the chemical reagents. The aromatic epoxy prepolymers used were diglycidyl ethers of bisphenol A (DGEBA). The ratio of secondary hydroxyls to epoxy groups varies from 0.015 for DER 332 indicating, in that case, that the main present species are pure DGEBA (M = 340 g/mol, n = 0) to 0.245 for DER 337 indicating the presence of higher molecular weight oligomers. The viscosity range covered by the epoxy prepolymers goes from 5 to 11 Pa · s at 25°C when $\bar{n}$ goes from 0.03 to 0.15.

The comonomer used as curing agent was methyl tetrahydrophthalic acid anhydride (MTHPA). The cure mechanisms of epoxide/anhydride systems are very complex and not well known actually. It is assumed that the epoxy group is bifunctional and so is the cyclic anhydride. Thus for a diglycidyl ether of bisphenol A the functionality is equal to 4 and the stoichiometric ratio is calculated by the following formulæ:

$$r = \frac{2[\text{MTHPA}]}{4[\text{DGEBA}]}$$

The carboxy-terminated CTBN rubbers used were HYCAR 1300 × 8 and HYCAR 1300 × 13 (B. F. Goodrich). They have, respectively, a 18 and 26% acrylonitrile content and a number average molecular weight close to 3500 g · mol^{-1}. In order to avoid catalysis by COOH group, CTBN were refunctionalized with epoxy groups. Thus epoxy-terminated adducts (ETBN) with the epoxy monomer DGEBA $\bar{n}$ = 0.03 were prepared following a procedure previously described.[5] It essentially consists of an almost complete reaction of carboxyl groups with epoxides, using a carboxyl-to-epoxy ratio equal to 0.065 at 85°C in the presence of 0.18% by weight of triphenylphosphine. Due to the large excess of DGEBA $\bar{n}$ = 0.03, chain extension is low, so that the ETBN is at 90% a triblock copolymer DGEBA/CTBN/DGEBA and DGEBA blocks are linking to CTBN by the segment:

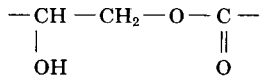

resulting from the reaction. ETBN were only used in the reactive systems comprising DGEBA $\bar{n}$ = 0.03.

The initiator introduced in the reactive systems was methyl imidazole (MIA). Previous studies[6] investigated the influence of various initiators (tertiary amines and different imidazoles) on the reactivity and the glass transition temperature of the final network. For 1% by weight of methyl imidazole, the highest value of the glass transition temperature was obtained for the anhydride-to-epoxy ratio r equal to 0.85. Thus these conditions were kept constant all during this study.

Cure Schedules

For each formulation, the appropriate amounts of the compounds were mixed and degassed at room

a) diglycidyl ether of bisphenol A (DGEBA) :

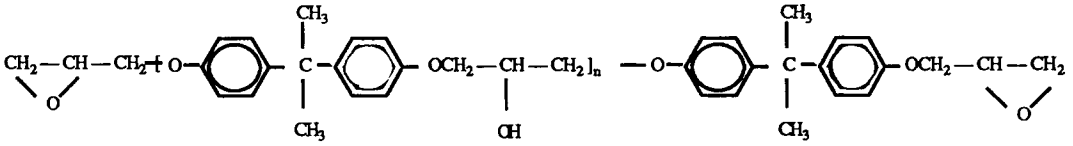

b) methyl tetrahydrophthalic anhydride (MTHPA) :

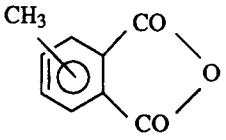

c) carboxy terminated butadiene acrylonitrile random copolymer (CTBN) :

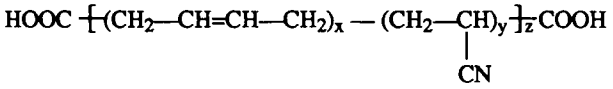

d) methyl imidazole (MIA) :

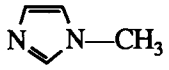

Figure 2 Structural formulæ of epoxy prepolymers, comonomer, initiator, and CTBN rubbers.

temperature under mechanical stirring for almost 2 h. The mixture was poured into a PTFE-coated mold, cured in a forced air oven for 1 h at 100°C and 5 h at 160°C, and then cooled to room temperature. Cure schedules were optimized in order to obtain the highest reaction extent and to reach the maximum value of the glass transition temperature noted $T_{g\infty}$.

Table I Characteristics of Reagents

	Supplier and Commercial Trade Names	$\overline{M_n}$ (g mol^{-1})	$\bar{n}$[a]	% AN[b]	$\eta_{25°C}$[c] (Pa s)	δ[d] (MPa)$^{1/2}$
DGEBA	Dow (DER 332)	342	0.03	—	5	20
	Rutgers (164)	380	0.15	—	11	19.8
	Dow (DER 337)	479	0.49	—	—	19.6
MTHPA	Anchor (Epiclon B570)	166	—	—	—	20.7
CTBN	B. F. Goodrich (Hycar 1300 × 8)	3600	—	18	150	17.9
	B. F. Goodrich (Hycar 1300 × 13)	3200	—	26	570	18.7

[a] Measured by size exclusion chromatography.
[b] Measured by microanalysis.
[c] Measured with Contraves Rheomat 30.
[d] Calculated by Hansen's method.

Experimental Techniques

Glass Transition Temperature Measurements

Glass transition temperatures T_g's were determined using differential scanning calorimetry (DSC) with a Mettler TA3000 apparatus. DSC specimens (10–20 mg) were heated from 0 to 250°C under an argon atmosphere with a heating rate of 10 $K \cdot min^{-1}$. T_g was taken as the temperature corresponding to the onset of heat capacity base-line change. Differential scanning calorimetry showed that, with the cure cycle used, the systems exhibited a constant glass transition temperature between two temperature scans.

Dynamic Mechanical Analysis

In the glass transition region, the dynamic shear modulus G^* (storage modulus G', loss modulus G'', and loss factor tan δ) was recorded as a function of temperature using a Rheometrics RDA 700 viscoelastimeter operating at 11 Hz. Rectangular specimens ($1.5 \times 6 \times 38$ mm^3) were tested in torsion mode from 30 to 200°C with a heating rate of 1 $K \cdot min^{-1}$.

In the β secondary relaxation region of the epoxy/anhydride matrix, the dynamic modulus E^* (E', E'', and tan δ) was recorded at 0.016 Hz using a Rheometrics RSA II system. The previously described specimens were tested in a double cantilever beam system from −140 to 50°C on temperature steps.

Elastic Properties

Young's moduli (E_{25}) at room temperature were obtained in tension mode using an Adamel Lhomargy DY25 testing machine. Dogbone H2 type specimens (length L_0 = 10 mm, width w = 4 mm, thickness t = 4 mm) were tested using an EX10 extensometer at a strain rate $\dot{\epsilon} = 1.67 \times 10^{-3}$ s^{-1}.

Yielding Behavior

The compression stress-strain curves were obtained with an Adamel Lhomargy DY25 testing machine equipped with a compression rig. Yield stresses (σ_y) were measured at room temperature at the strain rate of $\dot{\epsilon} = 8 \times 10^{-4}$ s^{-1}.

Linear Elastic Fracture Mechanics

Single-edge notched specimens (SEN) (thickness $t \approx 6$ mm and width $w \approx 12$ mm) were machined in plates and tested in three-point bending mode (span-to-length = 48 mm) at 25°C. Cracks of length a were made at ambient temperature using a diamond saw and finished with a razor blade at 155°C (above T_g). This short-time treatment above T_g had no effect on the properties of the networks since the cure was complete (see above). The crack length was measured by optical microscopy and was in the range 1–5 mm. About 12 notched specimens with various a/w were fractured (crosshead speed = 1 mm min^{-1}). The stress deflection curves are typical of a brittle fracture without stick-slip propagation.

The critical stress intensity factor (K_{Ic}) was calculated using the following formulæ:

$$K_{Ic} = \sigma_c \sqrt{\pi a}\, f(a/w)$$

where σ_c is the critical stress for crack propagation and $f(a/w)$ the form factor.[7]

The critical strain energy release rate G_{Ic} can be related to the stress-intensity factor K_{Ic} in plane-strain conditions by the equation

$$G_{Ic} = (K_{Ic}^2/E_{25})(1 - \nu^2)$$

where ν is the Poisson's coefficient and E_{25} the Young's modulus of the material · ν was measured with a two crossed-strain gauges (Vishay). For all formulations ν was equal to 0.33.

Fatigue

These tests were performed on the composites. At first we tested two composites in three-point bending mode to determine their load at break F_R.

Then the fatigue equipment permitted to test four composites in three points bending mode with an imposed deformation at room temperature and at a 5 Hz frequency. The deformation applied during the fatigue test was determined so that the initial applied force equaled to 0.35 F_R or 0.5 F_R. The load F was then recorded as a function of the number of cycles N imposed on the specimens. With the curves $F = f(N)$, the number of cycles N_{10} for which the strength has decreased from 10% can be obtained. The tests were stopped when N_{10} was higher than 10^6 cycles.

RESULTS AND DISCUSSION

Influence of the Average Molecular Weight of the Diepoxy Prepolymer DGEBA on the Processing and the Mechanical Properties of the Network

Increasing molecular weight of the DGEBA prepolymer from 342 to 479 g · mol^{-1} leads to an increase of the initial viscosity of the reactive liquid system from 0.5 to 2 Pa · s, keeping a pot life greater than 90 min at 27°C. If 0.5 Pa · s is too low, 2 Pa · s

is generally in the range of the correct viscosities used for filament winding processing.

The study of the kinetic mechanism during the polymerization of the reactive system is not the aim of this work; but as these mechanisms determine the formation and structure of the network and so its properties, the main results obtained in the literature are presented. The polymerization between an anhydride and an epoxy prepolymer in the presence of a base (in our case, methyl imidazole) is governed by an anionic mechanism that can be described by three stages.

(i) The initiation step:

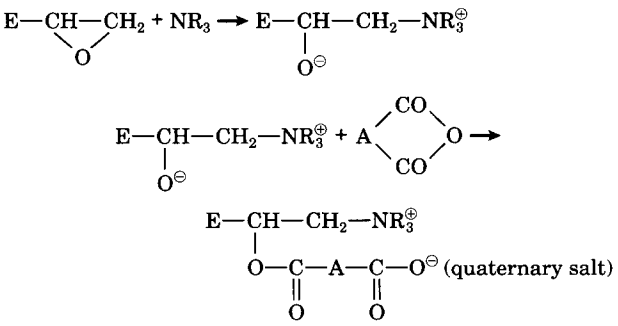

The quaternary salt will be noted

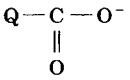

in the next formulæ.

(ii) The propagation step:

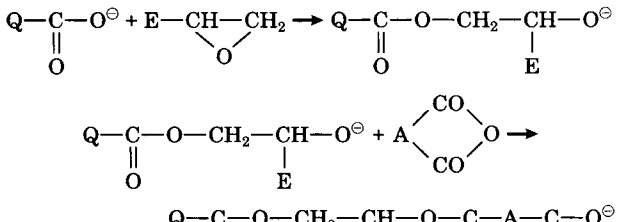

diester

(iii) Termination and transfer reactions with some compound containing active hydrogen (TH):

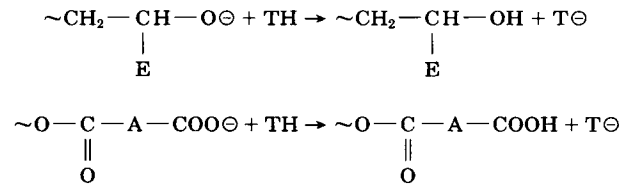

As can be seen, the base has not only an accelerating effect but also an initiating effect, and it can affect the chain length[8-10] and thus the properties of the networks. Another important fact is that, contrary to epoxy/amine step polymerization, network formation is not necessarily homogeneous. Indeed, as gelation can occur very early, the network formation process can be heterogeneous, and it is then possible to observe formation of microgels prior to the formation of a macrogel, leading to an heterogeneous network.

In the case of an homogeneous network, when all epoxy functions have reacted, the variations in crosslink density are only caused by differences in end group concentration of the resulting network, and a direct relation exists between T_g and $1/\overline{M_c}$, $\overline{M_c}$ being the average molecular weight between crosslinks.

In our case, another fact must be mentioned. We use an excess of epoxy groups and an homopolymerization could occur in presence of the imidazole. So the mechanisms involved during the formation of the networks are very complex. For this reason without kinetics informations, it is not possible to calculate the theoretical average molecular weight between crosslinks. Nevertheless, experimental $\overline{M_c}$ values have been calculated using the modulus G'_R, in the rubbery state. G'_R is measured at $T_m + 50°C$, T_m being the temperature at the tan δ maximum of the main α relaxation. The rubbery moduli stay in the same range and decrease slightly as the average molecular weight of the epoxy prepolymer increases. Experimental $\overline{M_c}$ values are calculated using the rubber elasticity theory:

$$\overline{M_c} = \frac{\rho R(T_m + 50)}{G'_R}\phi$$

where ρ is the density and ϕ the ratio of the mean square end-to-end distance of a network chain to that of a randomly coiled chain (it is called front factor).[11]

Assuming as usually done, ϕ equal to 1, the experimental values of $\overline{M_c}$ may be calculated and the results are presented in Table II. $\overline{M_c}$ increases as the molecular weight of the prepolymer DGEBA increases. This evolution can be related to the glass transition temperature (Table II). The relation between $T_{g\infty}$ and $1/\overline{M_c}$ is linear (Fig. 3), and the equation of the experimental straight line is

$$T_{g_\infty} = 55 + \frac{3.6 \times 10^4}{\overline{M_c}} \quad (°C)$$

Table II Characteristics of Networks Based on Anhydride and Various Molecular Weight DGEBA Prepolymers[a]

DGEBA	$\bar{n}$ = 0.03	$\bar{n}$ = 0.15	$\bar{n}$ = 0.49
$T_{g\infty}$ (°C)	135	133	125
E_{25} (GPa)	2.73 ± 0.08	2.5 ± 0.07	2.44 ± 0.07
σ_y (MPa)	110 ± 3	109 ± 3	108 ± 3
K_{Ic} (MPa · $\sqrt{m}$)	1.33 ± 0.04	1.31 ± 0.04	1.57 ± 0.05
G_{Ic} (J/m^2)	580 ± 35	610 ± 36	900 ± 54
G'_R (MPa)	9.5 ± 0.2	9.3 ± 0.2	8.12 ± 0.2
$\overline{M_c}$ exp(g · mol^{-1})	449	457	514

[a] $T_{g\infty}$ = glass transition temperature; E_{25} = Young's modulus; σ_y = compressive yield stress; K_{Ic} = critical stress intensity factor; G_{Ic} = critical strain energy release rate; G'_R = rubbery modulus (at T_m + 50°C); $\overline{M_c}$ = experimental average molecular weight between crosslinks.

This result is in accordance with the equation proposed by Nielsen,[12] $T_g - T_{g0} = (3.9 \times 10^4)/\overline{M_c}$. However, it is difficult to give a significance to the high value found for T_{g0} (T_{g0} = 55°C).

The evolution of the average molecular weight between crosslinks can also be related to mechanical properties and particularly to the critical strain energy release rate G_{Ic} (Table II). The variation of G_{Ic} reflects an increase in the toughness of the networks as the molecular weight of the DGEBA prepolymer is higher. This evolution cannot be attributed to the difference between the testing temperature (25°C) and the glass transition temperature of the networks. Indeed we observe a decrease of only 10°C between the glass transition temperature obtained, respectively, with DGEBA $\bar{n}$ = 0.03 and DGEBA $\bar{n}$ = 0.49.

We can also note that at 25°C all the networks are quite in the same state of mobility: The relaxation observed at −50°C by dynamic mechanical analysis at 11 Hz, relative to the secondary β relaxation of the epoxy anhydride networks[13,14] has almost the same amplitude for DGEBA $\bar{n}$ = 0.03 and for DGEBA $\bar{n}$ = 0.49 (Fig. 4) and the value of the Young's moduli E_{25} (Table II) stay in the same range (2.4–2.7 GPa). So the variation of G_{Ic} can only be explained by the difference between the average molecular weight between crosslinks of the networks. The evolution of G_{Ic} versus $\overline{M_c}^{1/2}$ is linear for our systems (Fig. 5), and numerous results in the literature show this same trend on epoxy–amine networks.[15–18]

If an increase of the number average molecular weight of the epoxy prepolymer leads to an improvement of fracture properties, it seems to have no effect on the plastic deformation. Indeed, the yield stress measured in compression at 25°C has roughly the same value for the three epoxy prepolymers used (Table II).

With this study, we have shown that increasing the average molecular weight of DGEBA prepolymer in anhydride-based systems leads to an increase of the initial viscosity of the liquid reactive system, in addition to an increase of the critical strain energy

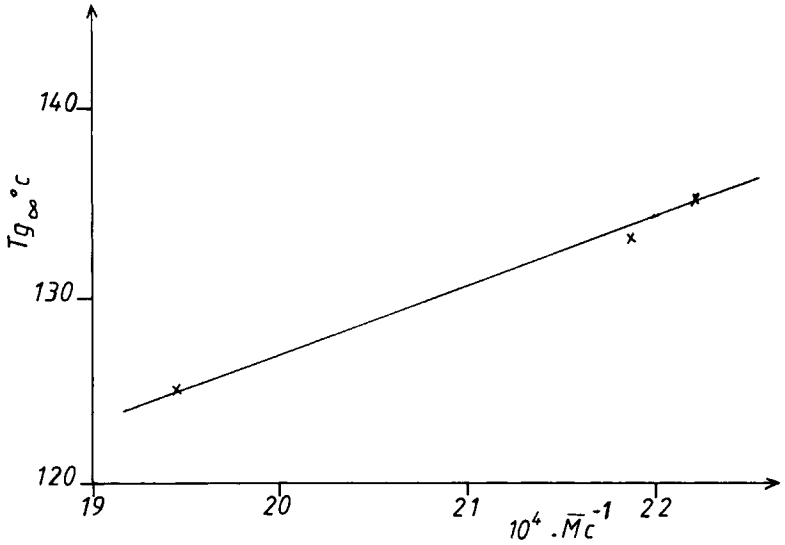

Figure 3 Relation between the glass transition temperature and the experimental average molecular weight between crosslinks for the networks modified by different-molecular-weight epoxy prepolymers.

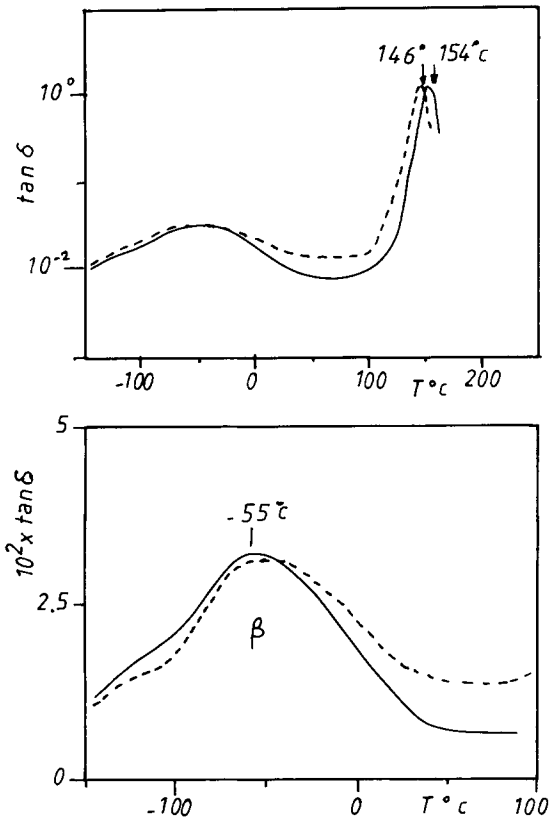

Figure 4 β-relaxation for (——) DGEBA $\bar{n}$ = 0.03/MTHPA/MIA and (- - - - -) DGEBA $\bar{n}$ = 0.49/MTHPA/MIA at 11 Hz.

release rate, keeping a high value for $T_{g\infty}$ ($T_{g\infty}$ = 125°C).

Influence of the Introduction of Rubber

The second way to increase the viscosity consists in introducing initially miscible elastomers in the basic system DGEBA $\bar{n}$ = 0.03/MTHPA/MIA. The chosen elastomers are epoxy-terminated butadiene–acrylonitrile rubbers (ETBN). In this study, we used two triblock copolymers, DGEBA–CTBN–DGEBA. The first one, ETBN13, is obtained from CTBN13 containing 26% AN and the second one, ETBN8, from CTBN8 containing 18% AN. These initially miscible elastomers are usually incorporated in epoxy formulations and particularly in epoxy–amine systems to lead to a phase separation phenomenon (with rubber particles from 0.1 to 5 μm dispersed in the rigid epoxy matrix) and so to improve impact resistance.

Few studies have been concerned in the literature with DGEBA/anhydride/CTBN systems and the results about phase separation are contradictory.[19-23] Hussain and Garry[19] and Visconti and Marchessault[22] clearly showed the presence of rubber domains of a few microns in size in CTBN-reinforced DGEBA/anhydride systems by means of SEM and light scattering, respectively.

Meeks[20] studied two anhydride-based networks modified by CTBN, but in this case no phase separation was evidenced by SEM. Finally, Zeng et al.[23] showed that the size of dispersed rubber particles depends on the type of elastomer introduced in the reactive epoxy/anhydride system. Thus adding a carboxyl-randomized butadiene–acrylonitrile copolymer leads to very small rubber domains (40–200 Å) and to networks that are still optically clear. If butadiene–acrylonitrile copolymer (without carboxyl contained) is added to this last system, the networks become opaque: The size of rubber particles increases. In a previous study,[24] the role of acrylonitrile content was also examined, and it was shown that increasing the acrylonitrile amount in rubber widens the range of miscibility of DGEBA/rubber blends.

In this paper, we will determine the influence of the acrylonitrile percentage in the case of anhydride based networks. So 5, 10, or 15 wt % rubbers [CTBN8 (18% AN) and CTBN13 (26% AN)] are introduced in the initial system DGEBA $\bar{n}$ = 0.03/MTHPA/MIA. In what follows, the butadiene acrylonitrile rubber (R) in the formulations will be expressed as a percentage mass fraction, indicated by % R, calculated from the initial CTBN content before any reaction has occured.

The stoichiometric ratio r = 0.85 is calculated considering the sum of epoxide functions from DGEBA monomer and rubber adduct. The viscosities of the reactive systems containing 10% R8 and

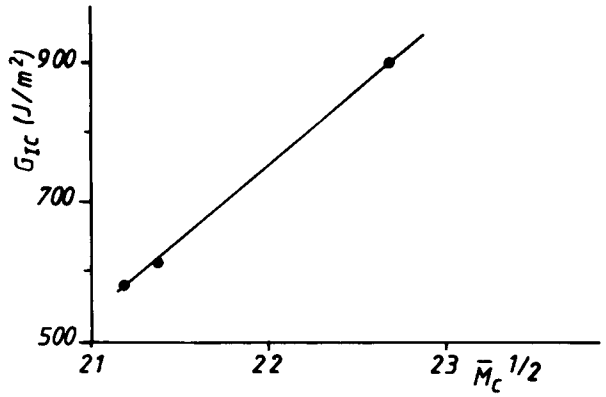

Figure 5 Relation between the critical strain energy release rate G_{Ic} and the experimental average molecular weight between crosslinks $\overline{M_c}$.

Table III Characteristics of the Rubber-Modified Epoxy–Anhydride Networks Compared to the Neat System[a]

Triblock Copolymer Type	None	ETBN13		ETBN8	
R (%)	0	5	10	10	15
${}_ET_{g\infty}$ (°C)	135	120	115	116	114
W_R (%)	0	5	6.7	5.3	5.9
E_{25} (GPa)	2.73 ± 0.08	2.6 ± 0.08	2.4 ± 0.07	2.25 ± 0.07	1.8 ± 0.05
σ_y (MPa)	110 ± 3	105 ± 3	97 ± 3	91 ± 3	75 ± 2
K_{Ic} (MPa · $\sqrt{\text{m}}$)	1.33 ± 0.04	1.28 ± 0.04	1.39 ± 0.04	1.56 ± 0.05	1.7 ± 0.05
G_{Ic} (J/m^2)	580 ± 35	560 ± 34	720 ± 43	1010 ± 60	1430 ± 86

[a] ${}_ET_{g\infty}$ = glass transition temperature of the networks; W_R = mass fraction of rubber dissolved in the matrix; and E_{25} = Young's modulus, σ_y = compressive yield stress, K_{Ic} = critical stress intensity factor, and G_{Ic} = critical strain energy release rate, all at 25°C.

10% R13 are respectively in the range 2–2.6 and 1.3–2 Pa s for the first 2 h at 27°C. Thus the optimum conditions for impregnation have been reached. The properties of the elastomer-modified networks are presented in Table III.

Generally, when the phase separation takes place, the final networks are cloud.[25] In our case they are always transparent for the two types of rubbers. The analysis of the cleaved surfaces by SEM does not show the presence of dispersed particles in the limit of uncertainty. TEM studies were not possible because the methyl tetrahydrophthalic acid anhydride has a carbon–carbon double bond (C=C). It is then impossible to mark only the rubber with OsO_4. Thus the remaining question is to know if there are dispersed rubber particles in our networks.

According to the study of Verchere et al.,[26] a viscoelastic analysis of the glassy state can bring information about the phase separation phenomenon. Indeed, on rubber-modified epoxy–amine networks, the distinction between β peak (relative to the secondary relaxation of the network) and α_R relaxation (relative to principal relaxation of the rubber) has been possible but only at a low frequency of measurement according to the difference between the apparent activation energy of a β and a α processes. Our networks have been studied at 0.016 Hz, and their dynamic mechanical behavior in the low temperature region clearly shows the main relaxation α_R associated with the glass transition of the elastomer.

For ETBN8, the relaxation α_R occurs at −66°C (T_{gR} measured by DSC was equal to −60°C), and at about −120°C we can see the secondary β relaxation peak of the epoxy/anhydride matrix [Fig. 6(a)]. On the ETBN13-modified epoxy–anhydride network [Fig. 6(b)] the main α_R relaxation of the elastomer has a very slight amplitude and occurs at −38°C (T_{gR} measured by DSC was equal to −42°C). This very low amplitude demonstrates that for the same R value a larger part of the elastomer is dissolved in the ETBN13-modified network than in the ETBN8-modified network. The initial better miscibility of ETBN13 (due to a higher content of acrylonitrile) to the epoxy/anhydride system can explain this observation.[24] Thus dynamic mechanical spectroscopy confirms that the rubber exists in the two cases as a dispersed phase in the epoxy/anhydride matrix, even if the rubber-modified networks exhibit only one glass transition temperature (Fig. 7).

We notice that increasing the initial rubber fraction from 0 to 10% decreases ${}_ET_{g\infty}$ value. In the range 10–15% R, ${}_ET_{g\infty}$ seems to be stable (${}_ET_{g\infty} \approx 115$°C). This evolution is very different from that obtained on epoxy–amine networks[27] (Fig. 7). Generally the decrease of ${}_ET_{g\infty}$ is attributed to the increase in the content of rubber dissolved in the matrix. As phase separation has been clearly evidenced by viscoelastic analysis and in order to estimate the amount of elastomer dissolved, the Fox equation may be applied[28]:

$$\frac{1}{{}_ET_{g\infty}} = \frac{1 - W_R}{T_{gE}} + \frac{W_R}{T_{gR}}$$

where W_R is the mass fraction of rubber dissolved in the matrix, T_{gE} = 135°C is the glass transition temperature of the pure matrix, and T_{gR} is the glass transition temperature of the pure rubber measured by DSC at the same scanning rate (T_{gR} = −60°C for CTBN8 and T_{gR} = −42°C for CTBN13).

The results obtained are presented in Table III. According to this calculation, W_R is in the range 5–7% and, for the same R value (10%), is slightly

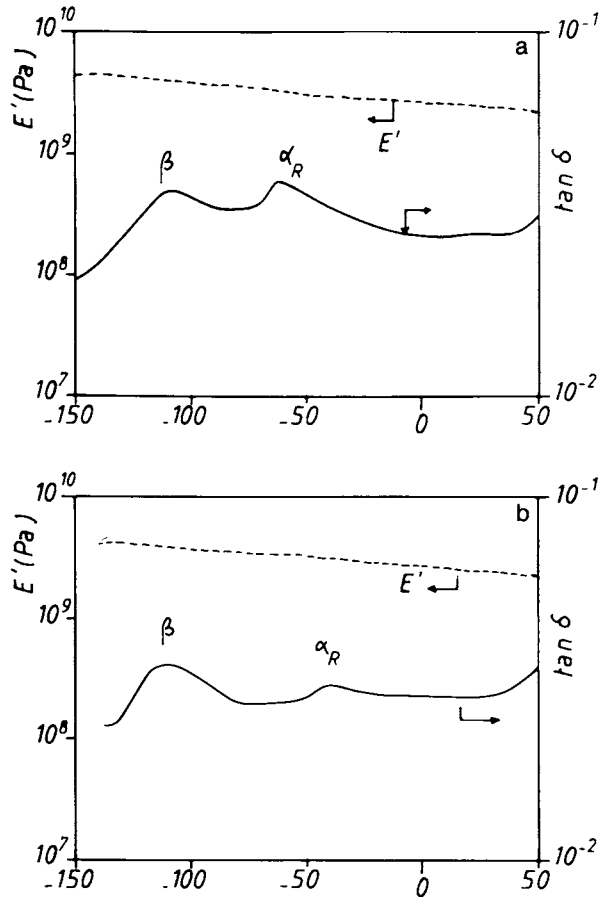

Figure 6 Dynamic mechanical spectra for rubber-modified epoxy/anhydride networks at 0.016 Hz: (a) for 15% R8; (b) for 10% R13.

higher for ETBN13 than for ETBN8, thus for the adduct containing the most important acrylonitrile content [W_R (10% R13) = 6.7% and W_R (10% R8) = 5.3%). Compared to the epoxy-amine networks studied by Verchere et al.,[24] for the same R value, the mass fraction of rubber dissolved in the anhydride-based matrix is more important than in the diamine-based matrix. The influence of the introduction of rubber on the mechanical properties of the networks is now characterized. The results are presented in Table III.

Introducing rubber in the anhydride matrix leads to an increase of the critical strain energy release rate G_{Ic}. This evolution is the result of the combined effects of the decrease of the Young's modulus and the increase of the critical stress intensity factor. The improvement of K_{Ic}, noted for 10% R13, is small (ΔK_{Ic} = 0.06 MPa · $\sqrt{m}$), and is more important for 10% R8 (K_{Ic} = 1.58 MPa · $\sqrt{m}$, ΔK_{Ic} = 0.25 MPa · $\sqrt{m}$), when the amount of rubber dissolved in the matrix is lower. As the rubber particles cannot be detected by SEM, it is not possible to discuss the role of the particle size in the failure mechanism implied during the fracture test.

The plastic behavior of the networks will now be examined. It generally has a great influence on the fracture resistance.[7] The compression stress–strain curves obtained at 25°C with the same strain rate ($\dot{\epsilon} = 8 \times 10^{-4}$ s^{-1}) exhibit a decrease in the yield stress σ_y as the initial amount of elastomer increases (Table III), showing the increasing ability of the networks to deform plastically. The decrease of σ_y can be related to the decrease of the glass transition temperature[29] as R is higher. The evolution of the critical stress intensity factor K_{Ic}, with the yield stress σ_y (Fig. 8) is in agreement with a previous study done by Kinloch and Young[7] for diamine-based epoxy networks with different stoichiometric ratios. Thus the introduction of CTBN type elastomers in the anhydride-based epoxy networks leads to an important increase of the critical strain energy release rate G_{Ic} and in addition to a small loss of the glass transition temperature (for 10% R, ${}_E T_{g\infty} \geq 115$°C). The transparency which permits the visual control of composite pieces is kept, despite the phase separation phenomenon that leads to the formation of very small rubber particles ($\bar{D} < 0.05$ μm).

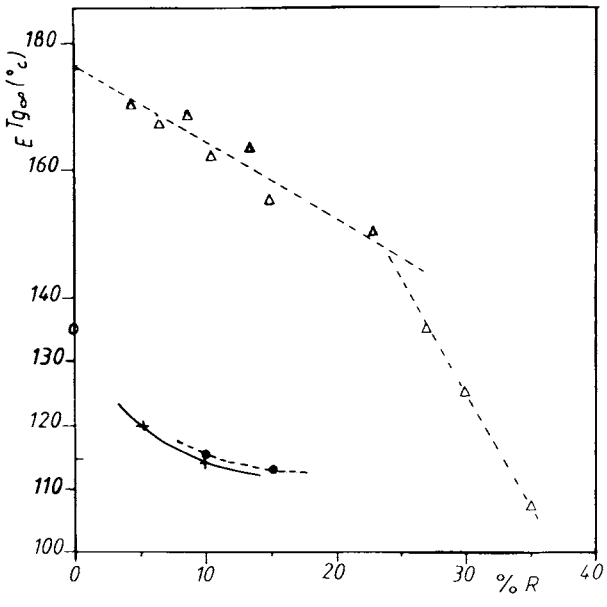

Figure 7 Variation of the glass transition temperature versus the weight percentage of rubber: (△) DGEBA $\bar{n}$ = 0.03/3DCM r = 1/R8; (●) DGEBA $\bar{n}$ = 0.03/MTHPA/MIA r = 0.85/R8; (+) DGEBA $\bar{n}$ = 0.03/MTHPA/MIA r = 0.85/R13.

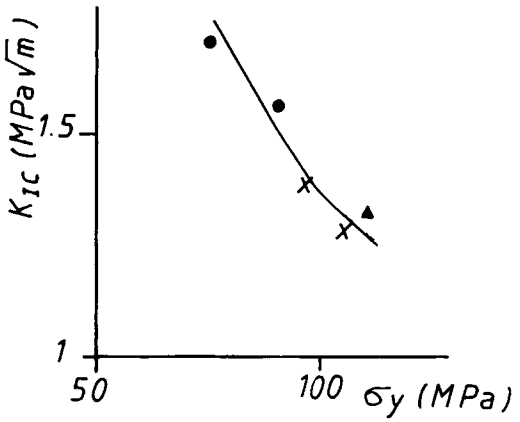

Figure 8 Critical stress intensity factor K_{Ic} as a function of the yield stress σ_y for the networks modified by introduction of elastomer: (▲) no rubber; (×) R13; (●) R8.

Application to Unidirectional Composites

If the role of elastomer is clear for improvements in static strength of composites, it is a controversial question in fatigue.[30] Hwang et al.[31,32] studied the fatigue resistance of epoxy networks toughened with two reactive liquid rubbers: an epoxy-terminated butadiene–acrylonitrile rubber (ETBN) and an amino-terminated butadiene–acrylonitrile rubber (ATBN). They show that rubber incorporation improves both impact and fatigue crack propagation resistance and that this last property is linearly proportional to $\overline{M_c}^{1/2}$. But are these conclusions still true in the case of fiber reinforced rubber modified matrices? The aim of our work is to apply the improvement of the matrix toughness to fiber-reinforced unidirectional composites tested in fatigue.

A preliminary study on epoxy/amine systems[33] permits selection of the appropriate glass fiber types (P103 from Vetrotex and a glass fiber type from Owens Corning Fiberglass) and shows that decreasing fiber content leads to an improvement of fatigue resistance of the composites in agreement with Fiore study.[34] The results obtained with epoxy–anhydride systems are presented in Table IV. At first we can see that the properties obtained with the same matrix (DGEBA $\bar{n}$ = 0.03/MTHPA/MIA/10% R8) and with the two types of fiber used are equivalent. Thus the comparison between all the composites will be possible.

We checked that the cure cycle applied to the composites permitted to obtain the optimum epoxy conversion (T_g values of the composites matrices are quite the same as for the corresponding networks). The role of the matrix on the fatigue behavior of the composites has now to be discussed:

(i) When the molecular weight of the diepoxy prepolymer increases, the fatigue resistance of the composites is higher. This is the result of two effects: the toughness improvement of the matrix and the decrease of the composites fiber content from 79 to 75% related to the modification of the matrix. Indeed, as we have seen during the first part of this study, replacing DGEBA $\bar{n}$ = 0.03 by a higher-molecular-weight DGEBA leads to an increase of the initial viscosity of the liquid reactive system. This has an influence on the fiber content of the final composite and on its fatigue resistance.[34]

(ii) In the case of introduction of elastomers we also noticed an increase of the fatigue resistance and in that case for a roughly constant fiber content. The best result (N_{10} higher than 10^6 cycles at 50% F_R) is ob-

Table IV Influence of the Matrix Modification on the Properties of the Unidirectional Composites[a]

	Vetrotex P103-2400 Tex			OCF 2400 Tex	
Reactive System	DGEBA $\bar{n}$ = 0.03 0% R	DGEBA $\bar{n}$ = 0.03 10% R13	DGEBA $\bar{n}$ = 0.03 10% R8	DGEBA $\bar{n}$ = 0.03 10% R8	DGEBA $\bar{n}$ = 0.49 0% R
T_g (°C)	127	112	114	114	124
Fiber content (% by weight)	79.5	77	77	77	75
F_R (da N)	197 ± 6	119 ± 4	112 ± 3	116 ± 3	132 ± 4
N_{10} at 50% F_R	6.5×10^5	6.6×10^5	$> 10^6$	$> 10^6$	$> 10^6$
N_{10} at 35% F_R	$> 10^6$	$> 10^6$	$> 10^6$	$> 10^6$	$> 10^6$

[a] T_g = glass transition temperature; F_R = static force at break in three points bending mode; N_{10} = number of cycles for which the force has decreased from 10% during the fatigue test.

tained with the matrix modified with 10% R8. It had a higher value of fracture toughness than the 10% R13 modified matrix.

Thus, in that case, the fatigue resistance of the composites seems strongly depend on the resistance to crack propagation of the matrix. The correlation between the matrix toughness and the fatigue composites behavior is complex as shown in the literature, especially in the case of glass fiber composite with rubber-reinforced matrices. If for Mandel et al.[35] the fatigue performance of glass fibre composites strongly depends on the fiber characteristics, for Giavotto[36] the matrix can also play an important role on the fatigue behavior of the composites.

In fact, the performance of the composites are determined by the relative strengths of the constituents.[37] So for composites with static failure strains greater than composite fatigue strain limits, the fatigue behavior is governed by matrix and interphase damage mechanisms. Otherwise, the fatigue performance of the composites are only governed by the fibre properties.

In our case the matrix performance has a great influence on the fatigue composites behavior especially in the case of rubber modified networks. This can be explained by the fact that the rubber particles formed during the polymerization are very small as we have seen in the second part of this study ($\bar{D} < 0.05$ μm). Thus their formation during polymerization is not perturbed by the presence of fibers, and after reaction they can entirely play their reinforcing role.

CONCLUSION

Increasing the average molecular weight of the epoxy prepolymer or introducing an epoxy-terminated butadiene acrylonitrile rubber has the following effects on the properties of an epoxy–anhydride formulation:

- the increase of the initial viscosity of the liquid reactive system
- the increase of the fracture toughness of the network accompanied by a small loss of the rigidity and of the glass transition temperature.

The mechanisms implied in the fracture properties reinforcement are different in function of the modifications types:

- A linear relationship is displayed between G_{Ic} and $\overline{M_c^{1/2}}$ as different average molecular weight epoxy prepolymers is used.
- The increasing ability of the networks to deform plastically is strongly related to the improvement of fracture properties in the case of rubber modified networks.

The introduction of ETBN leads to a phase separation phenomenon with very small rubber particles, not observed by SEM but the presence of a rubber phase was displayed by viscoelastic measurements. Indeed at low frequency the spectra clearly show the main relaxation α_R associated with the glass transition of the elastomer.

The two types of modified networks were used as fiber-reinforced composite matrices, and the fatigue behavior of those composites was evaluated. The results show an increasing fatigue life when DGEBA $\bar{n} = 0.49$ is used or when the matrix is reinforced by 10% R8, so when the matrices have a higher toughness.

This research was supported by Peugeot S. A. and the authors wish to thank MM. A. Gerard and G. André for their help during this study.

REFERENCES

1. M. A. Golub and N. R. Lerner, *J. Appl. Polym. Sci.*, **32,** 5215 (1986).
2. L. S. Penn and T. T. Chiao, *Natl. SAMPE Tech. Conf.*, **7,** 177 (1975).
3. E. Urbaczewski, J. P. Pascault, H. Sautereau, C. C. Riccardi, S. M. Moschiar, and R. J. J. Williams, *Makromol. Chem.*, **19,** 943 (1990).
4. C. K. Riew and J. K. Gillham, *J. Chem.*, **1984,** 372.
5. P. Bartlet, J. P. Pascault, and H. Sautereau, *J. Appl. Polym. Sci.*, **30,** 2955 (1985).
6. N. Bouillon, L. Tighzert, and J. P. Pascault, *J. Appl. Polym. Sci.*, **38,** 2103 (1989).
7. A. J. Kinloch and R. J. Young, in *Fracture Behavior of Polymers,* Applied Science Publishers, London, 1983.
8. L. Matejka, J. Lovy, S. Pokorny, K. Bouchal, and K. Dusek, *J. Polym. Sci.*, **21,** 2873 (1983).
9. K. Dusek, S. Lunak, and L. Matejka, *Polym. Bull.*, **7,** 145 (1982).
10. B. Steinmann, *J. Appl. Polym. Sci.*, **39,** 2005 (1990).
11. L. R. G. Treloar, in *The Physics of Rubber Elasticity,* 2nd ed., Oxford University Press, London, 1958.
12. L. E. Nielsen, *J. Macromol. Sci. Rev. Macromol. Chem.*, **C3,** 69 (1969).
13. M. Ochi, H. Iesako, S. Nakajima, and M. Shimbo, *J. Polym. Sci. Polym. Phys. Ed.*, **24,** 251 (1986).

14. M. Ochi, S. Zhu, and M. Shimbo, *Polymer,* **27,** 1569 (1986).
15. J. D. Lemay, B. J. Swetlin, F. N. Kelley, *J. Chem.,* **1984,** 165.
16. M. Fischer, in *Physical Mechanism in Polymer Fracture,* Lausanne, September 1988.
17. N. Amdouni, H. Sautereau, J. F. Gérard, and J. P. Pascault, *Polymer,* **31,** 1245 (1990).
18. R. A. Pearson and A. F. Yee, *J. Mater. Sci.,* 2571 (1989).
19. A. Hussain and F. J. Garry, *Toughening of Anhydride Cured Epoxy Resins,* MIT Press, Cambridge, MA, 1980, research report R80-2.
20. A. C. Meeks, *Polymer,* **15,** 675 (1974).
21. A. C. Meeks, *Br. Polym. J.,* **7,** 1 (1975).
22. S. Visconti and R. H. Marchessault, *Macromolecules,* **7,** 913 (1974).
23. Y. B. Zeng, L. Z. Zhang, W. Z. Peng, and Q. Yu, *J. Appl. Polym. Sci.,* **42,** 1905 (1991).
24. D. Verchere, J. P. Pascault, H. Sautereau, S. M. Moschiar, C. C. Riccardi, and R. J. J. Williams, *Polymer,* **30,** 107 (1989).
25. A. C. Soldatos and A. S. Burhans, *Adv. Chem. Ser.,* **99,** 531 (1971).
26. D. Verchere, J. P. Pascault, H. Sautereau, S. M. Moschiar, C. C. Riccardi, and R. J. Williams, *J. Appl. Polym. Sci.,* **42,** 701 (1991).
27. D. Verchere, Ph.D., INSA, Lyon, 1989.
28. T. G. Fox, *Bull. Am. Phys. Soc.,* **1,** 123 (1956).
29. C. G'Sell, D. Jacques, and J. P. Favre, *J. Mater. Sci.,* to appear.
30. P. T. Curtis, in *Advanced Composites,* I. K. Partridge, Ed., Elsevier, London, 1989.
31. J. F. Hwang, J. A. Manson, R. W. Hertzberg, G. A. Miller, and L. H. Sperling, *Polym. Eng. Sci.,* **29,** 1466 (1989).
32. J. F. Hwang, J. A. Manson, R. W. Hertzberg, G. A. Miller, and L. H. Sperling, *Polym. Eng. Sci.,* **29**(20), 1477 (1989).
33. E. Urbaczewski, Ph.D., INSA, Lyon, 1989.
34. L. Fiore, Ph.D., Ecole Centrale, Lyon, 1988.
35. J. F. Mandell, D. D. Huang, and F. J. McGarry, *Comput. Technol. Rev.,* **3,** 96 (1981).
36. V. Giavotto, V. Wagner, M. Caslini, and C. Zanotti, *Proc. 14th ICAF Conf.,* 503 (1987).
37. O. Konur and F. L. Matthews, *Composites,* **20,** 317 (1989).

Received September 6, 1991
Accepted April 22, 1992